Phthalocyanine-BODIPY dye: synthesis, characterization, and utilization for pattern recognition of CYFRA 21-1 in whole blood samples

Raluca-Ioana Stefan-van Staden, Ionela Raluca Comnea-Stancu, Hülya Yanık, Meltem Göksel, Anghel Alexandru & Mahmut Durmuş

Analytical and Bioanalytical Chemistry

ISSN 1618-2642
Volume 409
Number 26

Anal Bioanal Chem (2017)
409:6195-6203
DOI 10.1007/s00216-017-0560-y

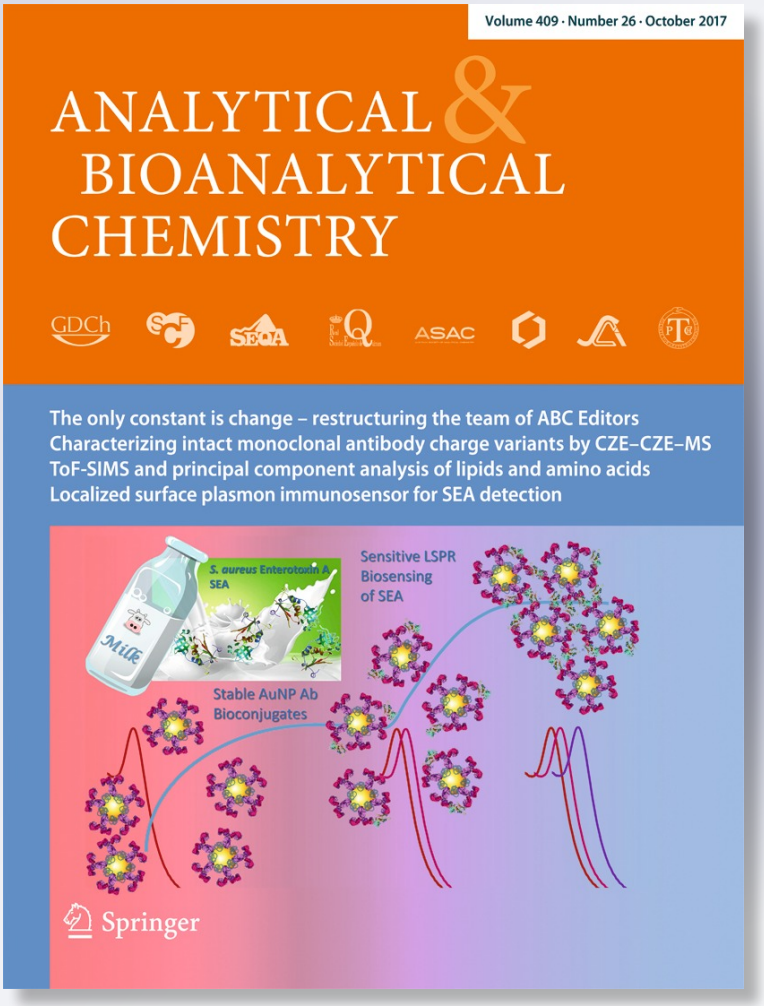

Springer

Anal Bioanal Chem (2017) 409:6195–6203
DOI 10.1007/s00216-017-0560-y

RESEARCH PAPER

Phthalocyanine-BODIPY dye: synthesis, characterization, and utilization for pattern recognition of CYFRA 21-1 in whole blood samples

Raluca-Ioana Stefan-van Staden[1,2] · Ionela Raluca Comnea-Stancu[1,2] · Hülya Yanık[3] · Meltem Göksel[3,4] · Anghel Alexandru[5] · Mahmut Durmuş[4]

Received: 16 April 2017 / Revised: 13 July 2017 / Accepted: 1 August 2017 / Published online: 29 August 2017

Abstract Phthalocyanine-BODIPY dye (BODIPY = boron dipyrromethene) was synthesized, fully characterized, and used for molecular recognition of CYFRA 21-1, a lung cancer biomarker, from whole blood samples. Thin films of three magnesium oxides ($(MgO)_n$, where n = 8, 9, or 10)) were deposited on a paper substrate, and they were immersed in a solution of phthalocyanine-BODIPY dye (1.17×10^{-3} mol/L) for the design of stochastic sensors. Limits of determination of picograms per milliliter magnitude order were recorded for the proposed stochastic sensors. CYFRA 21-1 was reliably identified and determined with recoveries higher than 95% and RSD lower than 1% in whole blood samples.

Keywords CYFRA 21-1 · Stochastic sensors · Lung cancer · Phthalocyanine · BODIPY

Electronic supplementary material The online version of this article (doi:10.1007/s00216-017-0560-y) contains supplementary material, which is available to authorized users.

✉ Raluca-Ioana Stefan-van Staden
ralucavanstaden@gmail.com

[1] Laboratory of Electrochemistry and PATLAB Bucharest, National Institute of Research for Electrochemistry and Condensed Matter, 202 Splaiul Independentei St., 060021 Bucharest, Romania

[2] Faculty of Applied Chemistry and Materials Science, Politehnica University of Bucharest, 1-7 Polizu St., 011061 Bucharest, Romania

[3] Department of Chemistry, Gebze Technical University, PO Box 141, 41400 Gebze, Kocaeli, Turkey

[4] Kosekoy Vocational School, Kocaeli University, PO Box 141, 41135 Kartepe, Kocaeli, Turkey

[5] Low Temperature Plasma Laboratory, National Institute for Lasers, Plasma and Radiation Physics (NILPRP), 409 Atomistilor St., 077125 Magurele, Romania

Introduction

CYFRA 21-1, a fragment of cytokeratin 19, is a tumor marker relatively new in the laboratory practice since the 1990s. It was first detected in nonsmall cell lung cancer, especially squamous cell carcinoma [1–4]. After then, it has been introduced as a potential marker for monitoring various types of diseases, including head and neck carcinoma [5, 6], esophageal cancer [7], bladder cancer [8], cervical cancer [9, 10], preeclampsia [11], biliary tract cancer (BTC) [12], intrahepatic cholangiocarcinoma (ICC) [13], breast cancer [14, 15], liver cancer [16], thyroid cancer [17, 18], undifferentiated nasopharyngeal carcinoma [19], and ovarian cancer [20–22].

Cytokeratins are part of the cytoskeleton of the epithelium. Previous studies identified 20 different cytokeratins and classified them into type I (acidic) and type II (neutral to basic) [13, 23, 24]. Serum CYFRA 21-1 is an acid-type cytokeratin with a molecular weight of 40 kDa that is released out of cells in the form of soluble fragments [25]. Expression of cytokeratin is altered during epithelial differentiation, and it is important for modulation and control of cell-cycle regulation and tumor cell apoptosis [26, 27].

To date, there were several methods reported for the assay of CYFRA 21-1 in biological fluids, including ELISA [5, 12, 22, 28], electrochemiluminescent immunoassay (ECLIA) [8, 11, 29], chemiluminescence immunoassay (CLIA) [30–32], radioimunoassay (RIA) [33, 34], and immunoradiometric assay (IRMA) [18, 27] (Table 1). The main disadvantages of these methods were laborious sampling, specialized equipments and personal involvement needed, and longtime analysis. Therefore, electrochemical methods that do not need any or minimum sample preparation and require easy-to-use instrumentation are of high interest for biomedical analysis [37].

In this paper, we proposed three stochastic sensors based on a phthalocyanine-BODIPY dye immobilized on ceramic

Table 1 Other methods proposed to date for the assay of CYFRA 21-1

Reference	Method	Detection limit (ng/mL)	Linear concentration range (ng/mL)	Type of sample
[30]	CLIA	0.20	0.2–50	–
[8]	ECLIA	0.10	1.18–460.7	Serum, urine
[32]	CLIA	0.01	0.9–71.4	Serum
[28]	ELISA	0.60	–	Serum, pleural fluid
[18]	IRMA	0.05	–	Serum
[35]	On-bacterium flow cytometric immunoassay	0.25	0–25	Serum
[36]	Two-step sandwich immunoassay (streptavidin-biotin technique)	0.10	–	Serum
[37]	Field effect transistor-based biosensor	1.00	1–1000	Serum

matrices, for the determination of CYFRA 21-1 from whole blood samples. Stochastic sensors are promising tools for biomedical analysis providing an alternative to the classical methods, due to their high reliability in identifying and quantifying the analytes in complex samples. The principle of stochastic sensors is based on channel/pore conductivity [38, 39]: on the first stage, the molecule is entering the channel/pore and is blocking it; the conductivity of the channel is dropping to zero; the time taken by the molecule to enter the channel (signature of the analyte) is depending only on the size, geometry of the molecule, and on its capability of unfolding and its speed to enter the channel, and it is not depending on the type and nature of the matrix; therefore, it is difficult to find two molecules with the same signature (t_{off} value). The second stage is strictly related to the quantitative measurements.

Because in biomedical analysis the first important issue is to perform a reliable qualitative analysis, one should consider the stochastic sensors as the best choice for this analysis, because they can perform (based on the signatures of the analytes) a reliable qualitative analysis. Phthalocyanines are excellent nanostructured materials, able to provide stable channels/pores, and therefore are preferred versus other similar nanostructured materials for the design of such sensors.

Experimental

Reagents and materials

Dimethyl formamide, ethanol, $CuSO_4 \cdot 5H_2O$, and sodium ascorbate were purchased from Aldrich. Reaction was monitored by thin layer chromatography (TLC) using 0.25 mm silica gel plates with UV indicator ($60F_{254}$). Column chromatography was performed on silica gel 60 (0.04–0.063 mm), and preparative thin layer chromatography was performed on silica gel $60PF_{254}$. The polyoxy substituted zinc(II) phthalocyanine (**1**) [40] and 4,4′-difluoro-8-(4-propynyloxy)-phenyl-1,3,5,7-tetramethyl-4-bora-3a,4a–diaza-s-indacene (**2**) [41] were synthesized and purified according to the literature procedures.

CYFRA 21-1 (human cytokeratin 19 protein) was purchased from Abcam (MA, USA). Deionized water obtained from a Millipore Direct-Q 3 System (Molsheim, France) was used for the preparation of all standard solutions. Standard solution of different concentrations (2×10^{-3} pg/mL to 20 μg/mL) was prepared by serial dilution method.

Instrumentation

Elemental analyses data were obtained from Thermo Finnigan Flash 1112 Instrument. Infrared spectrum of compound **3** was recorded on a Perkin Elmer Spectrum 100 spectrophotometer. Electronic absorption spectra were measured on a Shimadzu 2101 UV-Vis spectrophotometer. Fluorescence excitation and emission spectra were recorded on a Varian Eclipse spectrofluorometer using 1 cm path length cuvette at room temperature. ^{1}H-NMR spectrum of compound **3** was recorded on a Varian 500-MHz spectrometer with tetramethylsilane (TMS) as an internal standard and chemical shifts (δ) are given in parts per million. The mass spectrum was obtained on a BRUKER Microflex LT by matrix-assisted laser desorption ionization-time-of-flight mass spectrometer (MALDI-TOF) technique using 2,5-dihydroxybenzoic acid (DHB) as a matrix.

A PGSTAT 12 potentiostat/galvanostat was connected to a three-electrode cell (working electrode—the new developed stochastic sensor, Ag/AgCl—reference electrode, and Pt wire—counter electrode) and linked to a computer via an Eco Chemie (Metrohm, Switzerland) software version 4.9. Chronoamperometry was employed for all measurements.

Synthesis

*Phthalocyanine-BODIPY dye (**3**)*

A mixture of compound **1** (15 mg, 7.11×10^{-3} mmol), 4,4′-difluoro-8-(4- propynyloxy)-phenyl-1,3,5,7-tetramethyl-4-

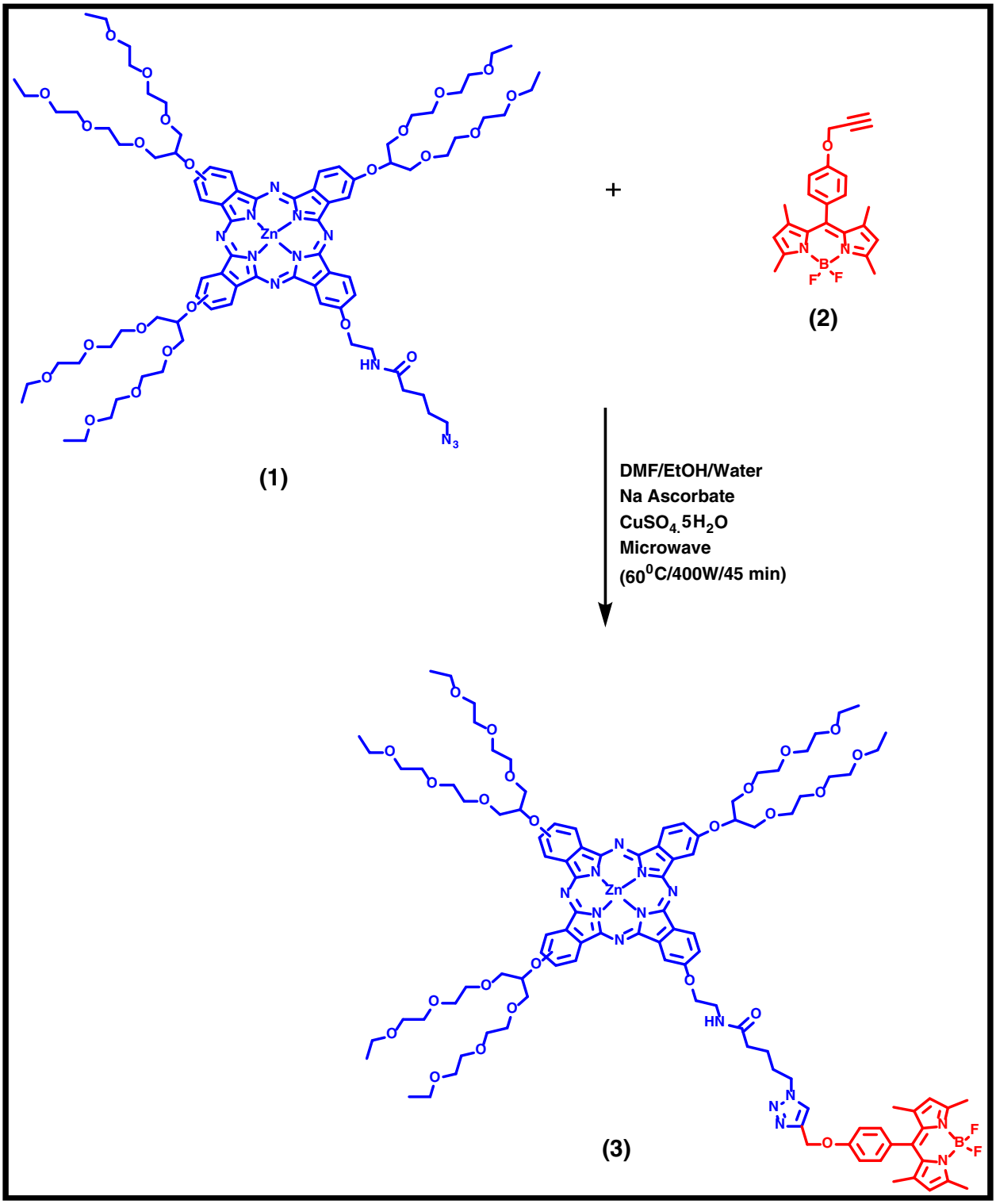

Fig. 1 Synthesis route of phthalocyanine-BODIPY dye **3**

bora-3a,4a–diaza-s-indacene (**2**) (5.38 mg, 1.43×10^{-2} mmol), $CuSO_4 \cdot 5H_2O$ (0.2 mg, 8.68×10^{-5} mmol), and sodium ascorbate (0.17 mg, 8.68×10^{-5} mmol) in a 12:1:1 mixture of DMF, ethanol, and water (5 mL) was stirred in a microwave oven at 400 W for 45 min (Fig. 1). After this time, the mixture was extracted with dichloromethane/water mixture. The organic phase was dried by anhydrous sodium sulfate and then filtered. Dichloromethane was evaporated until dryness. The

Table 2 Deposition parameters used for MgO coatings on paper by TVA plasma

Sample	$I_{filament}$ (A)	$I_{discharge}$ (A)	$U_{discharge}$ (V)	Anode-substrate distance (cm)
$(MgO)_8$	25	3	800	39
$(MgO)_9$				30
$(MgO)_{10}$				20

green residue was purified by silica gel column chromatography, using CH_2Cl_2/EtOH (20:1) solvent system as an eluent. Yield: 10 mg, 67%. FT-IR (υ_{max}/cm^{-1}): 3068 (aromatic CH), 2927–2865 (aliphatic CH), 1655 (C=C), 1492 (triazole), 1094 (C-O-C). Calc. for $C_{106}H_{139}B_1F_2N_{14}O_{24}Zn$ C 60.41, H 6.65, N 9.30%; found C 60.26, H 6.79, N 9.93%. ^{1}H-NMR (500 MHz, DMSO-d_6) δ ppm: 1.47 (6H, s, CH_3), 2.09 (18H, m, CH_3), 2.40 (6H, s, CH_3), 2.45 (8H, br, CH_2), 2.68–3.02 (4H, d-d, CH_2), 3.51–3.73 (72H, m, CH_2), 4.39 (3H, m, CH), 5.21 (2H, br, CH_2), 6.18 (2H, s, pyrrole-H), 7.07–7.31 (12H, m, aromatic CH), 7.33 (1H, br, triazole-H), 7.48 (1H, br, NH), 7.67–8.32 (4H, m, aromatic CH). MALDI-TOF-MS *m/z*: calc. 2107.51; found 2223.60 $[M\text{-}2F+DHB]^+$. UV/Vis: (DMSO, 1×10^{-5} M), λ_{max}/nm (log ε): 685 (5.16), 617 (4.73), 504 (4.68), 348 (5.04). Fluorescence (DMSO, 2×10^{-6} M), λ_{em}/nm: 508, 695.

Design of the stochastic sensors

Thin films of three magnesium oxides ($(MgO)_n$, where n = 8, 9, or 10) were deposited on a paper substrate with a length of 4 cm and a width of 2 mm, using the Thermionic Vacuum Arc (TVA) technique. TVA is a plasma-based coating method characterized by igniting a high voltage-high current discharge between a hot filament (cathode) and an anode consisting of the deposition material. In this case, the anode consisted of a TiB_2 boat filled with MgO powder. Base chamber pressure of 4×10^{-5} Torr was the same in all coating runs along with the plasma electrical parameters, while the only difference between them stands in the anode-substrate distance as presented in Table 2.

These thin films (Fig. 2) were immersed in a solution of phthalocyanine-BODIPY dye (1.17×10^{-3} mol/L) for 10 min and then left to dry at room temperature for 24 h. Before each measurement, the sensors were cleaned with deionized water. These sensors were stored in a dry and dark place at room temperature when they were not used.

Stochastic method

A chronoamperometric technique was selected for the stochastic sensing. All measurements were made at 125 mV versus Ag/AgCl. The electrodes were dipped into a cell containing standard solutions of different concentrations of CYFRA 21-1. The values of t_{on} were read on the recorded diagrams, and the equation of calibration $1/t_{on} = f(\text{conc.})$ was calculated using statistics (linear regression method). The unknown concentrations of CYFRA 21-1 in whole blood samples were determined by introducing the value of $1/t_{on}$ obtained after the measurements of samples in the equation of calibration.

Sample preparation

The University Emergency Hospital from the University of Medicine and Pharmacy "Carol Davila" Bucharest provided the whole blood samples from patients that were diagnosed with lung cancer, and control samples (healthy patients). The procedure for sample collection was in accordance with ethics committee approval no. 11/2013; informed consent was obtained from all patients. The samples did not need any pretreatment before the assay and were analyzed immediately after they were collected from the patients. The apparatus cell was filled with the whole blood sample, and the unknown concentration of the biomarker in whole blood samples was determined using the stochastic method described above.

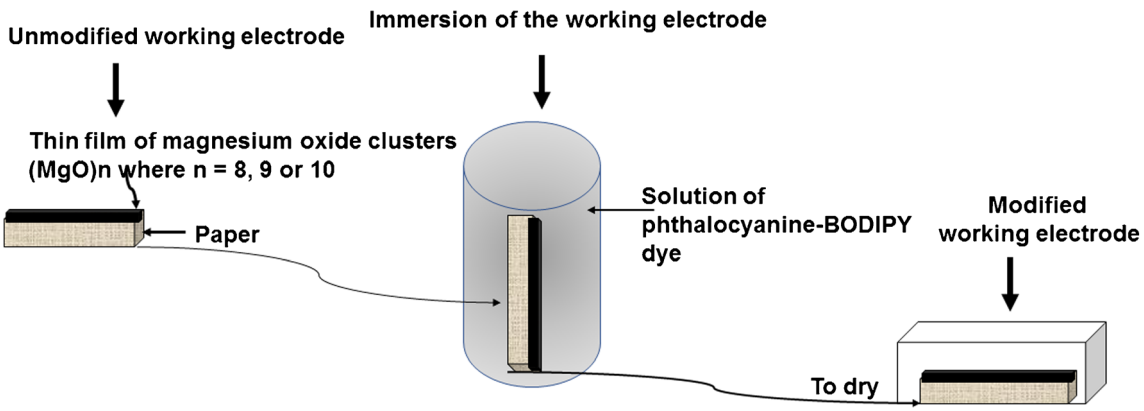

Fig. 2 Design of the stochastic sensors

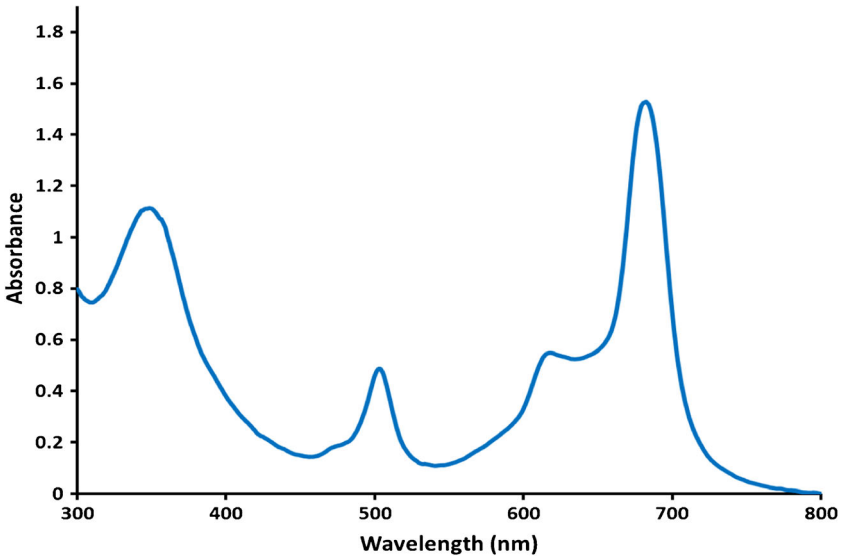

Fig. 3 UV-Vis absorption spectra of phthalocyanine-BODIPY dye (**3**) in DMSO ($C = 1 \times 10^{-5}$ M)

Results and discussion

Synthesis and characterizations

The asymmetrically polyoxy substituted zinc(II) phthalocyanine (**1**) [40] and 4,4′-difluoro-8-(4-propynyloxy)-phenyl-1,3,5,7-tetramethyl-4-bora-3a,4a–diaza-s-indacene (**2**) [41] were synthesized and purified according to the literature procedures. The asymmetrically substituted phthalocyanine compound **1** was conjugated with a BODIPY compound **2** via "click coupling" reaction using $CuSO_4{\cdot}5H_2O$ and sodium ascorbate as catalysts (Fig. 1).

In the FT-IR spectrum of phthalocyanine-BODIPY dye **3** (see Electronic supplementary material (ESM) Fig. S1), the aromatic CH vibration peaks were observed at 3068 cm^{-1}, and the aliphatic CH vibration peaks were observed between 2927 and 2865 cm^{-1}. The characteristic C-O-C vibration peak of polyoxy groups was observed at 1094 cm^{-1}. The N_3 stretching peak of the phthalocyanine compound **1** at 2096 cm^{-1} disappeared after the reaction of this phthalocyanine with BODIPY derivative **2** by the "click reaction." On the other hand, a novel vibration peak was observed at 1492 cm^{-1} for triazole ring on the phthalocyanine-BODIPY dye **3**.

The molecular ion peak of phthalocyanine-BODIPY conjugate (**3**) was observed at m/z 2226.60 as $[M+3K+2H]^+$ in the MALDI-TOF spectrum of this compound.

The presence of phthalocyanine aggregation at the concentrations used for the NMR measurements may lead to

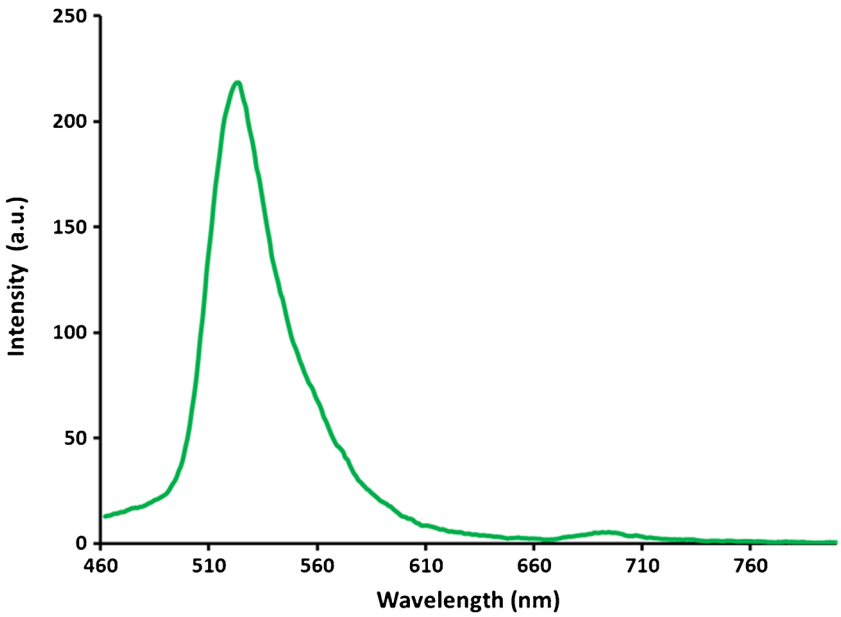

Fig. 4 Fluorescence emission spectrum of phthalocyanine-BODIPY dye (**3**) in DMSO (excitation wavelength = 450 nm)

Table 3 Response characteristics of the stochastic sensors used for the screening of CYFRA 21-1

Sensor based on phthalocyanine-BODIPY dye (**3**) and	t_{off} (s)	Linear concentration range (mg/mL)	Sensitivity (s mg^{-1} mL)	Equation of calibration[a]
$(MgO)_8$	2.6	2×10^{-4} to 2×10^{-2}	1.26	$1/t_{on} = 0.042 + 1.26 \times C$; $r = 0.9999$
$(MgO)_9$	2.1	2×10^{-6} to 2×10^{-4}	1.88×10^2	$1/t_{on} = 0.030 + 1.88 \times 10^1 \times C$; $r = 0.9999$
$(MgO)_{10}$	1.5	2×10^{-10} to 2×10^{-7}	2.61×10^5	$1/t_{on} = 0.056 + 2.61 \times 10^5 \times C$; $r = 0.9999$

[a] $<C>$ = mg/mL; $<t_{on}>$ = s

broadening of the aromatic signals. In the ^{1}H-NMR spectra of phthalocyanine-BODIPY conjugate (**3**) in DMSO-d_6, the aromatic protons of BODIPY unit were observed between 7.67 and 8.32 ppm. The proton signals on the amide and triazole groups were observed at 7.48 and 7.33 ppm as broad peaks, respectively. The protons belonging to the phthalocyanine core were observed between 7.07 and 7.31 ppm. The pyrrolic protons were observed at 6.18 ppm as a singlet band. The CH protons on the bridge of the polyoxy group were observed at 4.39 ppm. The aliphatic CH_2 protons were observed between 5.21 and 2.45 ppm. The aliphatic CH_3 protons of polyoxy groups were observed at 2.09 ppm as a multiplet peak. The aliphatic CH_3 protons on the BODIPY moiety were observed at 2.40 and 1.47 ppm as singlet peaks.

The characteristic absorption bands for both BODIPY and phthalocyanine moieties on the phthalocyanine-BODIPY dye **3** were observed at 504 and 685 nm which is an indication of the conjugation of phthalocyanine and BODIPY groups. Additionally, a broad peak was observed at around 348 nm due to the superimposition of the BODIPY absorption and B band absorption of the phthalocyanine core (Fig. 3). The fluorescence emission behavior of phthalocyanine-BODIPY dye **3** conjugate was determined in DMSO, and two emission maxima were observed at 508 and 695 nm for BODIPY and phthalocyanine moieties, respectively, when it excited at 450 nm (Fig. 4).

Response characteristics of the stochastic sensors used for the screening of CYFRA 21-1

Three stochastic sensors based on phthalocyanine-BODIPY dye **3** were used for the screening of whole blood samples for CYFRA 21-1. The response of the sensors was based on current conductivity: on the first stage, CYFRA 21-1 is blocking the channel and the current is dropping to zero until the molecule is entering the channel—the time spent on the first stage is called the signature (t_{off}) of CYFRA 21-1. The second stage is related to quantitative measurement of the concentration of CYFRA 21-1—and the binding process with the wall of the channel is taking place:

$$\mathrm{Ch}_{(i)} + \mathit{CYFRA}\,21\text{-}1_{(i)} \Leftrightarrow \mathrm{Ch}\bullet\mathit{CYFRA}\,21\text{-}1_{(i)}$$

where Ch is the channel and i is the interface, followed by redox processes; the time spent in the channel by CYFRA 21-1 is called t_{on} and its value is used for the quantitative evaluation of it in whole blood samples (Fig. 4). The response characteristics of the sensors used for the screening of CYFRA 21-1 are presented in Table 3. The best response was shown by the sensor based on $(MgO)_{10}$-**3** with a linear domain from 0.20 to 200 pg/mL, reaching a determination limit of 0.20 pg/mL. The proposed sensors were stable over a period of 6 months, when they were used daily for measurements; the RSD values recorded for the slopes of the calibration graphs were lower than 1.00%.

Selectivity of the sensors

The signatures obtained for different biomarkers (analytes) are given the selectivity of the proposed method. Therefore, other biomarkers used for lung cancer diagnosis, such as NSE, HER-1, HER-2, CA 199, and CEA, were measured, and different values for t_{off} (signatures) were obtained compared with the signature of CYFRA 21-1 reported in Table 3. Therefore, one can say that the proposed sensors are selective versus biomarkers that may interfere in the assay of CYFRA 21-1 in whole blood samples.

Analytical applications

The proposed stochastic sensors based on phthalocyanine-BODIPY dye **3** were used for the screening of whole blood samples for CYFRA 21-1 (Fig. 5). Qualitative assay of CYFRA 21-1 was performed based on its signature (t_{off} values), and the quantitative assay was done by introducing the values of t_{on} in the equations of calibration presented in Table 3.

Recovery tests were performed as the first step of method validation. Well-known volumes from solutions containing CYFRA 21-1 were added to 1 mL whole blood sample so that the concentrations are situated in the linear concentration range. Diagrams were recorded before and after the addition of the well-known volumes of the standard solution, and the concentrations found for CYFRA 21-1 were compared (Table 4) and reported as percentage from the added concentration. The obtained values show that the proposed sensors

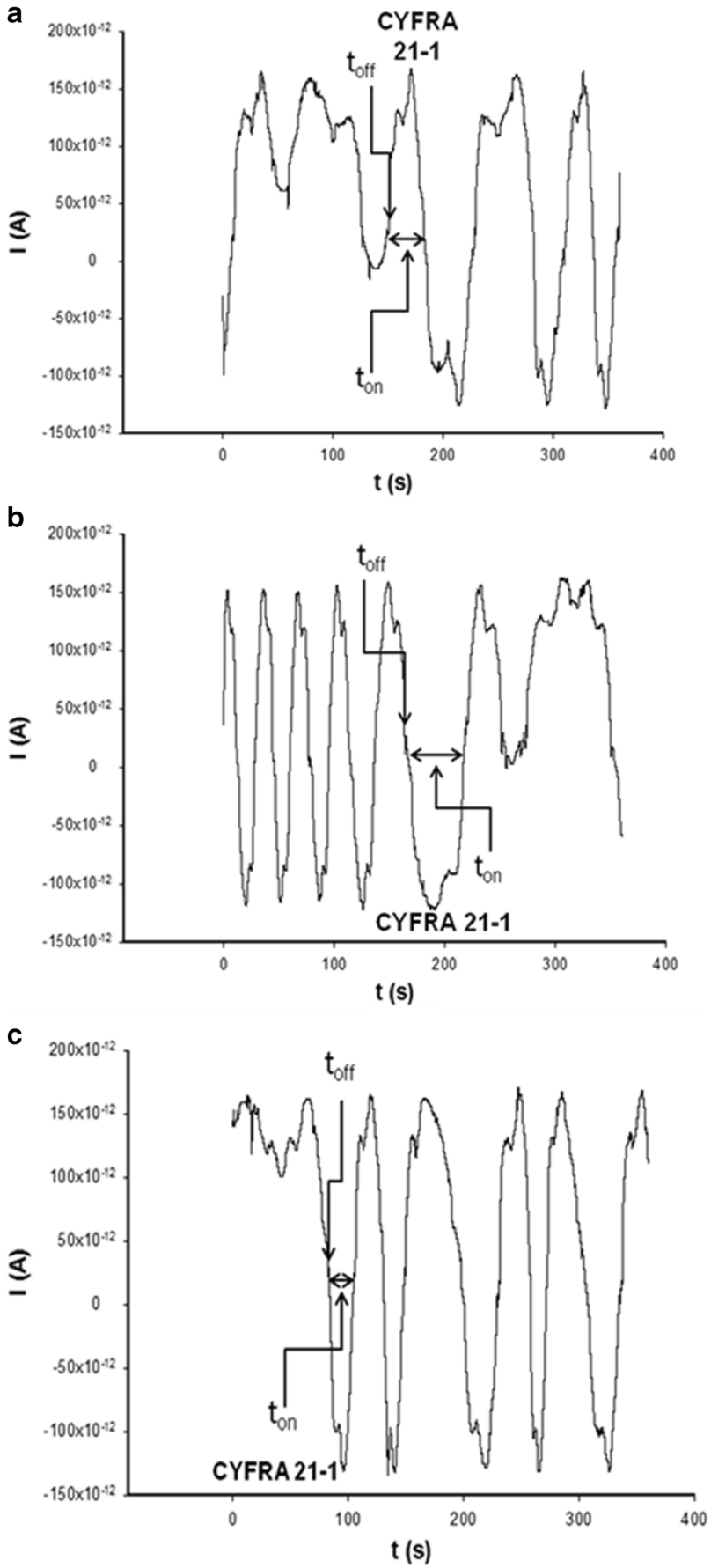

Fig. 5 Examples of diagrams recorded for the assay of CYFRA 21-1 in whole blood samples using stochastic sensors based on **a** $(MgO)_8$-**3**, **b** $(MgO)_9$-**3**, and **c** $(MgO)_{10}$-**3**>

Table 4 Assay and recovery test results for determination of CYFRA 21-1 in whole blood samples

Sample no.	CYFRA 21-1, recovery in whole blood samples, ng/mL			
	Sensor based on phthalocyanine-BODIPY dye (**3**) and			ELISA[a]
	$(MgO)_8$	$(MgO)_9$	$(MgO)_{10}$	
Control 1–10	_[b]	_[b]	_[b]	_[b]
1	27.75 ± 0.03	27.50 ± 0.02	27.48 ± 0.05	27.20 ± 0.48
2	69.60 ± 0.04	70.90 ± 0.03	70.03 ± 0.05	65.65 ± 0.45
3	8.86 ± 0.01	8.94 ± 0.02	8.95 ± 0.02	8.20 ± 0.43
4	154.10 ± 0.05	154.40 ± 0.08	153.82 ± 0.07	153.00 ± 0.48
5	107.30 ± 0.05	108.00 ± 0.05	108.33 ± 0.03	107.50 ± 0.53
6	14.95 ± 0.03	15.34 ± 0.03	15.18 ± 0.01	15.20 ± 0.75
7	22.60 ± 0.03	21.30 ± 0.02	21.53 ± 0.03	21.23 ± 0.53
8	88.75 ± 0.04	87.87 ± 0.04	87.96 ± 0.04	87.20 ± 0.43
9	41.90 ± 0.04	40.97 ± 0.02	41.82 ± 0.02	41.20 ± 0.55
10	195.52 ± 0.08	195.00 ± 0.05	195.05 ± 0.07	195.45 ± 0.75
11	8.91 ± 0.02	8.95 ± 0.01	8.81 ± 0.01	8.00 ± 0.57
12	27.90 ± 0.03	27.50 ± 0.02	27.41 ± 0.03	26.95 ± 0.70
Recovery, %	97.75 ± 0.02	99.96 ± 0.03	96.25 ± 0.03	–

[a] Standard method ($N = 5$)

[b] CYFRA 21-1 was not found in any control sample tested

can be used reliably for the assay of CYFRA 21-1 in blood samples.

A control sample (from a healthy patient) as well as whole blood samples from patients diagnosed with lung cancer was screened using the proposed sensors. CYFRA 21-1 was not found in the whole blood sample. The obtained results showed a good correlation among the results obtained using the three sensors (Table 4) as well as between these values and those obtained using a standard method (ELISA).

Conclusions

Phthalocyanine-BODIPY dye was synthesized and used as a modifier for magnesium oxide-free films. Immobilization of phthalocyanine-BODIPY dye **3** on magnesium oxides proved to produce reliable surfaces for the design of stochastic sensors with features for early detection of lung cancer. High sensitivity and low limit of determination were recorded using these sensors. The proposed sensors were designed to be disposable in order to avoid suspicion of cross contamination from one patient to another.

Acknowledgements This work was supported by a project within the frame PNII, Ideas 123/2011. IR Comnea-Stancu is thankful for the funding from the Sectorial Operational Programme Human Resources Development 2007–2013 of the Ministry of European Funds through Financial Agreement POSDRU/159/1.5/S/132395.

Compliance with ethical standards

Conflict of interest The authors declare that they have no conflicts of interest.

References

1. Pujol JL, Grenier J, Daures JP, Daver A, Pujol H, Michel FB. Serum fragment of cytokeratin subunit 19 measured by Cyfra 21-1 immunoradiometric assay as a marker of lung cancer. Cancer Res. 1993;53:61–6.
2. Takada M, Masuda N, Matsuura E, Kusunoki Y, Matui K, Nakagawa K, et al. Measurement of cytokeratin 19 fragments as a marker of lung cancer by CYFRA 21-1 enzyme immunoassay. Br J Cancer. 1995;71:160–5.
3. Pujol JL, Molinier O, Ebert W, Daures JP, Barlesi F, Buccheri G, et al. CYFRA 21-1 is a prognostic determinant in non-small-cell lung cancer: results of metaanalysis in 2063 patients. Br J Cancer. 2004;90:2097–105.
4. Park SY, Lee JG, Kim J, Park Y, Lee SK, Bae MK, et al. Preoperative serum CYFRA 21-1 level as a prognostic factor in surgically treated adenocarcinoma of lung. Lung Cancer. 2013;79:156–60.
5. Doweck I, Barak M, Uri N, Greenberg E. The prognostic value of the tumour marker Cyfra 21-1 in carcinoma of head and neck and its role in early detection of recurrent disease. Br J Cancer. 2000;83:1696–701.
6. Wang YX, Hu D, Yan X. Diagnostic accuracy of Cyfra 21-1 for head and neck squamous cell carcinoma: a meta-analysis. Eur Rev Med Pharmacol Sci. 2013;17:2383–9.
7. Yan HJ, Wang RB, Zhu KL, Jiang SM, Zhao W, Xu XQ, et al. Cytokeratin 19 fragment antigen 21-1 as an independent predictor for definitive chemoradiotherapy sensitivity in esophageal squamous cell carcinoma. Chin Med J. 2012;125:1410–5.
8. Jeong S, Park Y, Cho Y, Kim YR, Kim HS. Diagnostic values of urine CYFRA21-1, NMP22, UBC, and FDP for the detection of bladder cancer. Clin Chim Acta. 2012;414:93–100.

9. Aggarwal P, Kehoe S. Serum tumour markers in gynaecological cancers. Maturitas. 2010;67:46–53.
10. Sheng X, Du X, Zhang X, Li D, Lu C, Li Q, et al. Clinical value of serum HMGB1 levels in early detection of recurrent squamous cell carcinoma of uterine cervix: comparison with serum SCCA, CYFRA21-1, and CEA levels. Croat Med J. 2009;50:455–64.
11. Kuessel L, Wild J, Haslacher H, Perkmann T, Ristl R, Zeisler H, et al. Urine and serum concentrations of cytokeratin 19 in pre-eclampsia. Eur J Obstet Gynecol Reprod Biol. 2014;181:311–5.
12. Chapman MH, Sandanayake NS, Andreola F, Dhar DK, Webster GJ, Dooley JS, et al. Circulating CYFRA 21-1 is a specific diagnostic and prognostic biomarker in biliary tract cancer. J Clin Exp Hepatol. 2011;1:6–12.
13. Malaguarnera G, Paladina I, Giordano M, Malaguarnera M, Bertino G, Berretta M. Serum markers of intrahepatic cholangiocarcinoma. Dis Markers. 2013;34:219–28.
14. Nakata B, Ogawa Y, Ishikawa T, Ikeda K, Kato Y, Nishino H, et al. Serum CYFRA 21-1 one of the most reliable tumor marker for breast carcinoma. Cancer. 2000;89:1285–90.
15. Nakata B, Takashima T, Ogawa Y, Ishikawa T, Hirakawa K. Serum CYFRA 21-1 (cytokeratin-19 fragments) is a useful tumor marker for detecting disease relapse and assessing treatment efficacy in breast cancer. Br J Cancer. 2004;91:873–8.
16. Uenishi T, Kubo S, Hirohashi K, Tanaka H, Shuto T, Yamamoto T, et al. Cytokeratin 19 fragments in serum (CYFRA 21-1) as a marker in primary liver cancer. Br J Cancer. 2003;88:1894–9.
17. Giovanella L, Treglia G, Verburg FA, Salvatori M, Geriani L. Serum cytokeratin19 fragments: a dedifferentiation marker in advanced thyroid cancer. Eur J Endocrinol. 2012;167:793–7.
18. Isic T, Savin S, Cvejic D, Marecko I, Tatic S, Havelka M, et al. Serum Cyfra 21.1 and galectin-3 protein levels in relation to immunohistochemical cytokeratin 19 and galectin-3 expression in patients with thyroid tumors. J Cancer Res Clin Oncol. 2010;136:1805–12.
19. Zhu WQ, Yu JM, Sun XD, Xie P, Kong L. Serum CYFRA21-1 as a prognostic marker for patients with undifferentiated nasopharyngeal carcinoma. Biomarkers. 2010;15:602–7.
20. Hasholzner U, Baumgartner L, Stieber P, Meier W, Hofmann K, Faten-Mohadam A. Significance of the tumor markers CA125 II, CA 72.4, ASA and CYFRA 21-1 in ovarian carcinoma. Anticancer Res. 1994;14:2743–6.
21. Gadducci A, Ferdeghini M, Cosio S, Fanucchi A, Cristofani R, Genazzani AR. The clinical relevance of serum CYFRA 21-1 assay in patients with ovarian cancer. Int J Gynecol Cancer. 2001;11:277–82.
22. Yurkovetsky Z, Skates S, Lomakin A, Nolen B, Pulsipher T, Modugno F, et al. Development of a multimarker assay for early detection of ovarian cancer. J Clin Oncol. 2010;28:2159–66.
23. Moll R, Franke WW, Schiller DL, Geiger B, Krepler R. The catalogue of human cytokeratins: patterns of expression in normal epithelia, tumors and cultured cells. Cell. 1982;31:11–24.
24. Moll R, Schiller DL, Franke WW. Identification of protein IT of the intestinal cytoskeleton as a novel type I cytokeratin with unusual properties and expression patterns. J Cell Biol. 1990;111:567–80.
25. Zhong LP, Zhu HG, Zhang CP, Chen WT, Zhang ZY. Detection of serum Cyfra 21-1 in patients with primary oral squamous cell carcinoma. Int J Oral Maxillofac Surg. 2007;36:230–4.
26. Paraio JM, Jorcano JL. Beyond structure: do intermediate filaments modulate cell signaling? BioEssays. 2002;24:836–44.
27. Wu HH, Wang PH, Yeh JY, Chen YJ, Yen MS, Huang RL, et al. Serum cytokeratin-19 fragment (Cyfra 21-1) is a prognostic indicator for epithelial ovarian cancer. Taiwan J Obstet Gynecol. 2014;53:30–4.
28. Romero S, Fernández C, Arriero JM, Espasa A, Candela A, Martín C, et al. CEA, CA 15-3 and CYFRA 21-1 in serum and pleural fluid of patients with pleural effusions. Eur Respir J. 1996;9:17–23.
29. Xu RH, Liao CZ, Luo Y, Xu WL, Li K, Chen JX, et al. Optimal cut-off values for CYFRA 21-1 expression in NSCLC patients depend on the presence of benign pulmonary diseases. Clin Chim Acta. 2015;440:188–92.
30. Luo JP, Qu SX, Liu JT, Wang B, Cai XX. Rapid detection of Cyfra 21-1 by optical-biosensing based on chemiluminescence immunoassay using bio-functionlized magnetic nanocomposites. Chin Sci Bull. 2013;58:2567–8.
31. Wang Q, Lu JB, Wu B, Hao LY. Expression and clinicopathologic significance of proteolysis-inducing factor in non-small-cell lung cancer: an immunohistochemical analysis. Clin Lung Cancer. 2010;11:346–51.
32. Patel JL, Erickson JA, Roberts WL, Grenache DG. Performance characteristics of an automated assay for the quantitation of CYFRA 21-1 in human serum. Clin Biochem. 2010;43:1449–52.
33. Hanagiri T, Sugaya M, Takenaka M, Oka S, Baba T, Shigematsu Y, et al. Preoperative CYFRA 21-1 and CEA as prognostic factors in patients with stage I non-small cell lung cancer. Lung Cancer. 2011;74:112–7.
34. Paone G, De Angelis G, Greco S, Portalone L, De Marchis L, Galluccio G, et al. Evaluation of response to chemotherapy in patients affected with non-small cell lung cancer by means of three tumour markers elaborated by discriminant analysis. Respir Med. 1997;91:361–7.
35. Lan WJ, Lan W, Wang HY, Yan L, Wang ZL. An on-bacterium flow cytometric immunoassay for protein quantification. J Pharm Biomed Anal. 2013;83:129–34.
36. Fujita J, Ohtsukib Y, Bandoha S, Takashimac H, Uedaa Y, Wua F, et al. Elevation of cytokeratin 19 fragment (CYFRA 21-1) in serum of patients with radiation pneumonitis: possible marker of epithelial cell damage. Respir Med. 2004;98:294–300.
37. Cheng S, Hideshima S, Kuroiwa S, Nakanishi T, Osaka T. Label-free detection of tumor markers using field effect transistor (FET)-based biosensors for lung cancer diagnosis. Sensors Actuators B Chem. 2015;212:329–34.
38. Bayley H, Cremer PS. Stochastic sensors inspired by biology. Nature. 2001;413:226–30.
39. Braha O, Walker B, Cheley S, Kasianowicz JJ, Song L, Gouaux JE, et al. Designed protein pores as components for biosensors. Cell Chem Biol. 1997;4:497–505.
40. Göksel M, Durmuş M, Atilla D. Synthesis asymmetrically peptide conjugated zinc(II) phthalocyanine and comparison photophsicochemical properties via different fluorophores effect. Inorg Chim Acta. 2017;456:95–104.
41. Atilgan S, Ozdemir T, Akkaya EU. Selective Hg(II) sensing with improved Stokes shift by coupling the internal charge transfer process to excitation energy transfer. Org Lett. 2010;12:4792–5.